Langmuir

Article

pubs.acs.org/Langmuir

# Platinum Nanoparticles Functionalized with Ethynylphenylboronic Acid Derivatives: Selective Manipulation of Nanoparticle Photoluminescence by Fluoride Ions

Peiguang Hu, Yang Song, Mauricio Daniel Rojas-Andrade, and Shaowei Chen*

Department of Chemistry and Biochemistry, University of California, 1156 High Street, Santa Cruz, California 95064, United States

Supporting Information

**ABSTRACT:** Platinum nanoparticles functionalized with 4-ethynylphenylboronic acid pinacol ester (Pt–EPBAPE) were successfully synthesized by a simple chemical reduction procedure. Because of the formation of conjugated metal–ligand interfacial linkages, the resulting nanoparticles exhibited apparent photoluminescence arising from the nanoparticle-bound acetylene moieties that behaved analogously to diacetylene derivatives. Interestingly, the nanoparticle photoluminescence was markedly quenched upon the addition of fluoride ions ($F^-$). In contrast, significantly less or virtually no change was observed with a variety of other anions such as $Cl^-$, $Br^-$, $I^-$, $NO_3^-$, $HSO_4^-$, $H_2PO_4^-$, $ClO_4^-$, $BF_4^-$, and $PF_6^-$. The high selectivity toward fluoride ion is most probably because of the strong specific affinity of the boronic acid moiety to fluoride. The formation of B–F bonds led to the conversion of $Bsp^2$ to $Bsp^3$, as manifested in $^{11}B$ NMR measurements, which impacted the intraparticle charge delocalization between the particle-bound acetylene moieties and hence the nanoparticle photoluminescence.

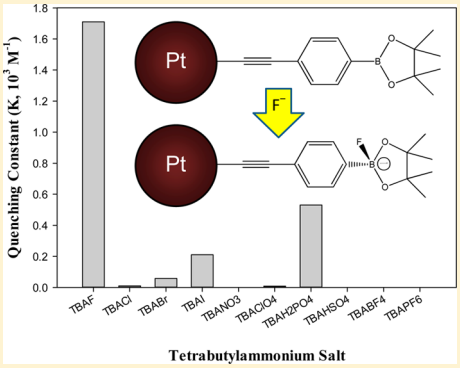


## INTRODUCTION

Organically capped transition-metal nanoparticles represent a unique class of functional materials that may be used as novel building blocks in diverse applications such as nanoelectronics, catalysis, and chemical and biological sensing.[1−5] This is largely motivated by the ready decoration of the nanoparticle surface with multiple/diverse functional moieties. In addition, the electronic interactions between the particle-bound functional moieties may be deliberately manipulated by the metal–ligand interfacial bonding interactions, leading to the emergence of unprecedented optical and electronic properties. In particular, it has been demonstrated that with conjugated metal–ligand interfacial bonds, extensive intraparticle charge delocalization occurs between the nanoparticle-bound functional moieties, which thus behave analogously to the dimeric counterparts.[6−10] For instance, for metal nanoparticles stabilized by the self-assembly of acetylene derivatives, the nanoparticles exhibit well-defined photoluminescence that is consistent with that of diacetylene derivatives.[9,11] More importantly, thanks to the extended conjugation within the nanoparticles, specific interactions of the nanoparticles with target analytes may lead to signal propagation/amplification and hence enhanced detection sensitivity, as manifested in the photoluminescence detection of nitroaromatics and lead ions ($Pb^{2+}$) by pyrene-functionalized ruthenium nanoparticles.[12,13] This is the primary motivation of the present study which is focused on the sensitive and selective manipulation of nanoparticle photoluminescence by deliberate functionalization of platinum nanoparticles with boronic acid derivatives that react selectively with fluoride ions ($F^-$).

The specific interactions between fluoride and boronic acid have been very well-known and used rather extensively for the development of chemical and biological sensors.[14−19] The general mechanism involves the formation of strong bonding between fluoride and boron that then leads to an apparent change of the fluorescence emission characteristics. Such a sensing architecture may be exploited for the sensitive and selective manipulation of nanoparticle optoelectronic properties with deliberate surface chemical functionalization. Within this context, in the present study, we prepared platinum nanoparticles functionalized with 4-ethynylphenylboronic acid pinacol ester which exhibited apparent photoluminescence that was consistent with those of diacetylene derivatives, thanks to the formation of conjugated Pt–C≡ bonds at the metal–ligand interface.[9,11] The boronic acid moieties served as the specific binding sites for fluoride ions, which exerted sensitive impacts on the nanoparticle photoluminescence. Importantly, the resulting nanoparticles exhibited excellent selectivity and sensitivity toward fluoride, in comparison with a series of other anions.

**Received:** January 10, 2014
**Revised:** March 10, 2014
**Published:** April 8, 2014

   dx.doi.org/10.1021/la5001123 | *Langmuir* 2014, 30, 5224–5229

## EXPERIMENTAL SECTION

**Chemicals.** Platinum chloride ($PtCl_2$, 98%, Alfa Aesar), 4-ethynylphenylboronic acid pinacol ester (EPBAPE, 95%, Sigma-Aldrich), tetra-*n*-octylammonium bromide (TOABr, 98%, Cole Parmer), tetrabutylammonium fluoride (TBAF, 98%, ACROS), tetrabutylammonium chloride (TBACl, ≥97%, ACROS), tetrabutylammonium bromide (TBABr, ≥98%, ACROS), tetrabutylammonium iodide (TBAI, ≥98%, ACROS), tetrabutylammonium nitrate ($TBANO_3$, 97%, ACROS), tetrabutylammonium hydrogen sulfate ($TBAHSO_4$, 97%, Aldrich), tetrabutylammonium dihydrogen phosphate ($TBAH_2PO_4$, 99%, Aldrich), tetrabutylammonium perchlorate ($TBAClO_4$, TCI America), tetrabutylammonium tetrafluoroborate ($TBABF_4$, ACROS), and tetrabutylammonium hexafluorophosphate ($TBAPF_6$, 98%, Fluka) were used as received. All solvents were obtained from typical commercial sources and used without further treatment. Water was supplied by a Barnstead Nanopure water system (18.3 MΩ·cm).

**Synthesis of Platinum Nanoparticles.** In a typical synthesis, 0.1 mmol of $PtCl_2$ were dissolved in a 1 mL concentrated HCl solution at 100 °C for 30 min. The solution was then cooled down to room temperature, into which was added 3 mL of a toluene solution of TOABr (0.1 M) under stirring for 1 h. The $H_2O$ phase was removed and the orange toluene phase was washed with $H_2O$ five times. The obtained toluene solution was reduced to 1 mL by blowing $N_2$, and 5 mL of THF as well as 0.3 mmol of EPBAPE was added into the toluene solution. Ten milligrams of $NaBH_4$ dissolved in 1 mL of ice-cold $H_2O$ was added into the solution dropwise under magnetic stirring. The appearance of a dark brown color signified the formation of platinum nanoparticles. The solution was stirred for 2 h before the solvents were removed by rotary evaporation. The obtained solids were rinsed with acetonitrile five times, affording purified platinum nanoparticles functionalized by the self-assembly of EPBAPE onto platinum surfaces, as depicted in Scheme 1A. The particles were denoted as Pt–EPBAPE and were found to be readily soluble in organic media such as dichloromethane and dimethylformamide (DMF).

**Scheme 1**

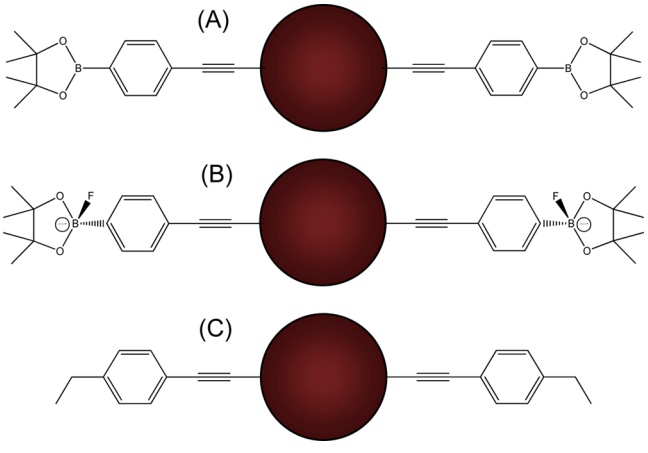


**Characterizations.** The morphology and sizes of the Pt–EPBAPE nanoparticles were characterized by transmission electron microscopic (TEM) studies (Philips CM300 at 300 kV). More than 200 nanoparticles were measured to obtain a size histogram. $^{11}B$ NMR spectroscopic measurements were carried out by using concentrated solutions of the nanoparticles in DMF-$d_6$ with a Varian Unity 500 MHz NMR spectrometer. Chemical shifts were referenced to $BF_3{\cdot}OEt_2$ in $CDCl_3$. FTIR measurements were carried out with a Perkin–Elmer FTIR spectrometer (Spectrum One, spectral resolution 4 $cm^{-1}$), where the samples were prepared by casting the particle solutions onto a ZnSe disk. Photoluminescence (PL) measurements were carried out with a PTI fluorospectrometer. Typically, 3 mL of a Pt–EPBAPE nanoparticle solution in DMF at a concentration of 0.01 mg/mL was added into a quartz cuvette. A series of calculated amounts of tetrabutylammonium salts (with different anions) were added into the cuvette by a Hamilton microliter syringe and the PL spectra were collected after thorough mixing of the nanoparticle solution.

## RESULTS AND DISCUSSION

Figure 1 depicts a representative TEM micrograph of the Pt–EPBAPE nanoparticles. It can be seen that the nanoparticles

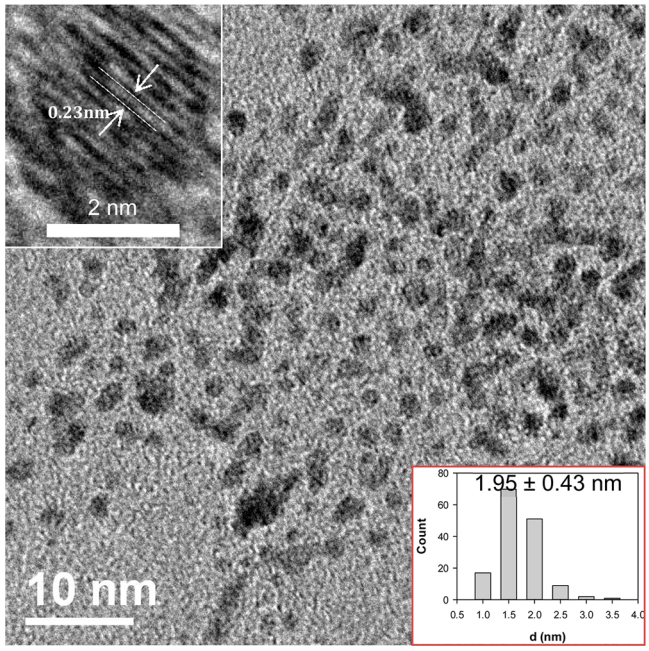


**Figure 1.** Representative TEM micrograph of Pt–EPBAPE nanoparticles. Scale bar 10 nm. Top inset shows a high-resolution image where the lattice fringes with a spacing of 0.23 nm can be identified. Bottom inset shows the corresponding core size histogram.

were very well dispersed without apparent agglomeration, suggesting sufficient protection of the nanoparticles by the EPBAPE ligands, as a result of the self-assembly of the acetylene moieties onto platinum nanoparticle surfaces forming Pt–C≡ bonds (Scheme 1A).[20] High-resolution imaging showed very well-defined lattice fringes with a spacing of 0.23 nm that are consistent with the (111) crystal planes of fcc Pt, as manifested in the top figure inset. Additionally, the core size histogram based on a statistical analysis of more than 200 nanoparticles shows that the majority of the nanoparticles are in the narrow range of 1.5 to 2.0 nm in diameter with an average of 1.95 ± 0.43 nm, as depicted in the lower inset.

The successful incorporation of the EPBAPE ligands onto the platinum nanoparticle surface was further manifested in FTIR measurements. Figure 2 depicts the FTIR spectra of the Pt–EPBAPE nanoparticles (black curve) and the monomeric EPBAPE ligands (red curve). It can be seen that, for the EPBAPE monomers, the terminal ≡C–H vibrational stretch can be clearly identified at 3291 $cm^{-1}$ and the C≡C stretch at 2108 $cm^{-1}$. Yet for the Pt–EPBAPE nanoparticles, the band at 3291 $cm^{-1}$ vanished, suggesting ready cleavage of the ≡C–H bonds upon the self-assembly of the ligands onto the Pt nanoparticle surface (this also indicates that the nanoparticles were free of excessive monomeric ligands). Meanwhile, the C≡C stretch was found to red-shift to 2046 $cm^{-1}$, which may be


dx.doi.org/10.1021/la5001123 | Langmuir 2014, 30, 5224–5229

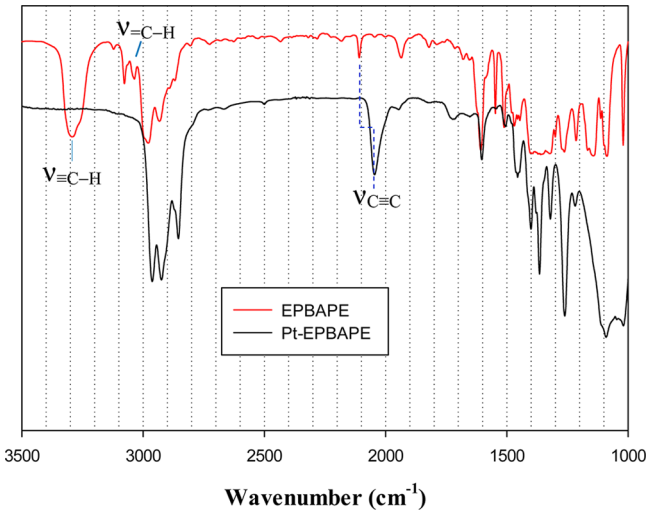


**Figure 2.** FTIR spectra of EPBAPE monomers (red curve) and Pt−EPBAPE nanoparticles (black curve).

ascribed to intraparticle charge delocalization as a result of the formation of conjugated Pt−C≡ interfacial bonds such that the particle-bound acetylene moieties behaved analogously to diacetylene derivatives (−C≡C−C≡C−) (additional contributions may arise from the formation of Pt−H bonds on the nanoparticle surface[21,22]). Furthermore, whereas the aromatic =C−H vibrations were rather apparent between 3000 and 3100 $cm^{-1}$ with the monomeric ligands, no vibrational features were observed above 3000 $cm^{-1}$ with the Pt−EPBAPE nanoparticles. This may also be accounted for by the intraparticle charge delocalization where the =C−H vibrations red-shifted and became overlapped with the methyl vibrations (2800−3000 $cm^{-1}$)——notably, the peak at 2850 $cm^{-1}$ became substantially intensified. Similar behaviors have also been observed previously with nanoparticles functionalized with other acetylene derivatives.[20]

Because of extensive intraparticle charge delocalization, the resulting Pt−EPBAPE nanoparticles exhibited apparent PL characteristics, akin to diacetylene derivatives.[20] As depicted by the black curves in Figure 3, despite a low concentration of only 0.01 mg/mL in DMF, the Pt−EPBAPE nanoparticles display an intense well-defined excitation peak at 335 nm and an emission one at 406 nm. Interestingly, from panel (A), one can see that, upon the addition of TBAF, the Pt−EPBAPE nanoparticles exhibited an apparent diminishment of the photoluminescence. For instance, at a TBAF concentration of 0.67 mM, the PL intensity of the Pt−EPBAPE nanoparticles decreased by more than 40%. Similar but much less drastic diminishments were observed in the presence of $TBAH_2PO_4$ and TBAI, as depicted in panels (B) and (C), respectively. In contrast, virtually no change of the nanoparticle PL was seen with the addition of TBABr (panel D) and other tetrabutylammonium salts that included TBACl, $TBANO_3$, $TBAClO_4$, $TBAHSO_4$, $THABF_4$, and $TBAPF_6$ (Figure S1 in the Supporting Information). These observations suggest high sensitivity and selectivity of the nanoparticle PL to fluoride ions.

Notably, with the addition of a large excess of TBAF, the emission intensity at 406 nm exhibited further diminishment and concurrently a new emission peak started to emerge at a

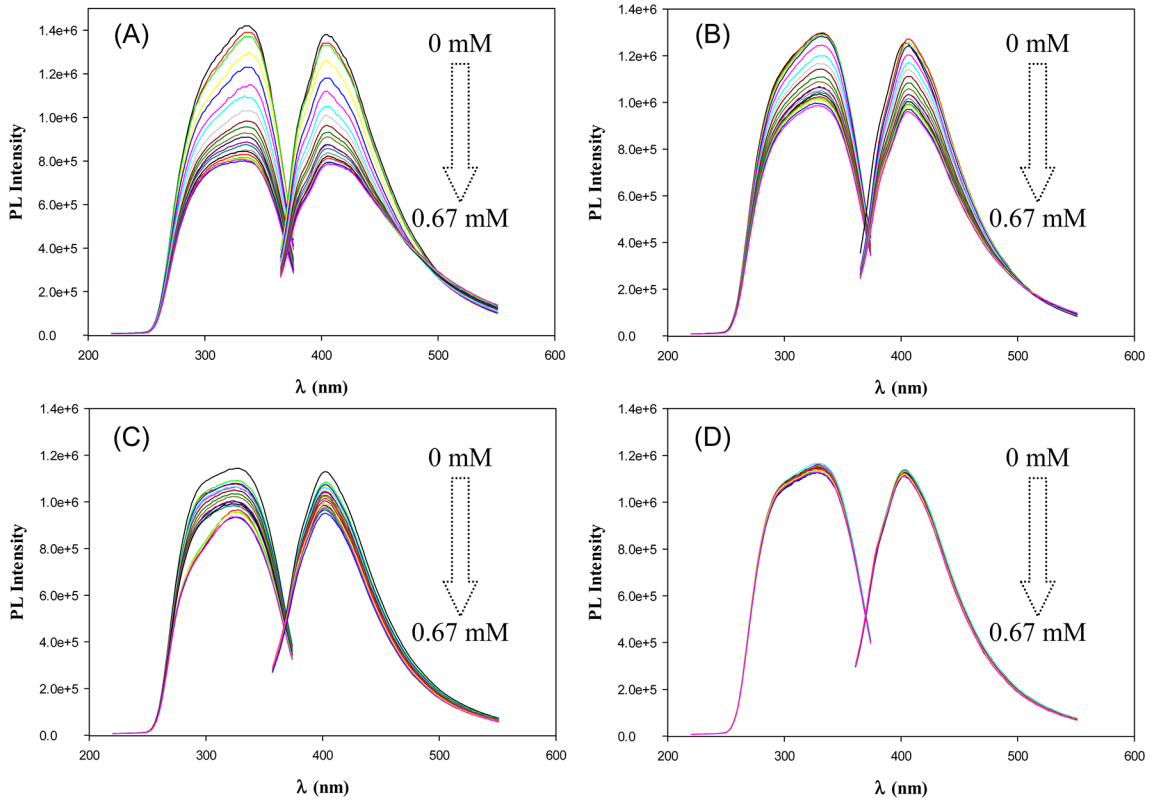


**Figure 3.** Excitation and emission spectra of Pt−EPBAPE nanoparticles in the presence of tetrabutylammonium salts at various concentrations up to 0.67 mM (concentration increment 33 μM): (A) TBAF, (B) $TBAH_2PO_4$, (C) TBAI, and (D) TBABr. Initial concentration of the nanoparticles was 0.01 mg/mL in DMF.


dx.doi.org/10.1021/la5001123 | *Langmuir* 2014, 30, 5224−5229

longer wavelength position of 460 nm and the intensity increased accordingly, leading to the appearance of an isoemission point around 435 nm in the emission profiles (Figure 4). In a previous study of ratiometric fluorescence

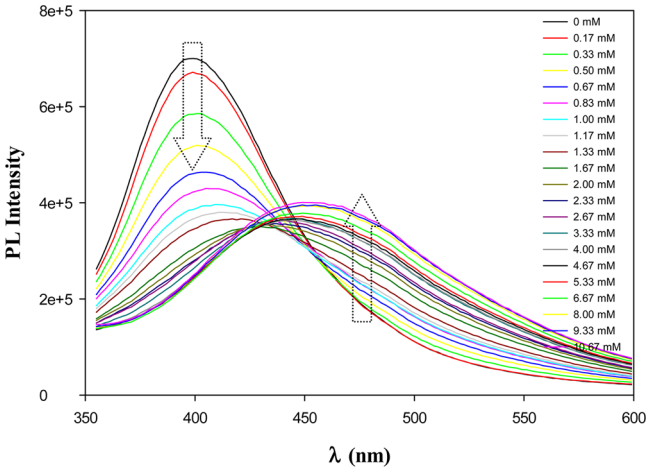


**Figure 4.** Photoluminescence emission spectra of Pt–EPBAPE nanoparticles (6 $\mu$g/mL in DMF) with the addition of TBAF up to 10.67 mM. Excitation wavelength was set at 335 nm.

sensing of fluoride ions by an asymmetric bidentate receptor containing a boronic acid and imidazolium group,[19] an isoemission point was clearly identified at 406 nm in acetonitrile with the addition of various amounts of fluoride ions. This may be ascribed to the unique interactions between fluoride ions and the $sp^2$ B in the boronic acid moieties of Pt–EPBAPE.[18,19,23−27] As shown in Scheme 1A, the B atom of the EPBAPE ligand possesses an $sp^2$ trigonal planar geometry with an empty p orbital perpendicular to the plane of the phenyl ring, allowing the boron atom to be conjugated with the phenyl carbons and hence involved in the intraparticle charge delocalization between the particle-bound acetylene moieties. Note that the boron atoms of such a feature are good electron receptors (nucleophiles) and the binding of fluoride ions into the vacant site most likely induces a change of the molecular geometry and hybridization of the boron atoms to $sp^3$, as shown in Scheme 1B. The $sp^3$ boron is no longer able to participate in the conjugation between the particle-bound phenylacetylene groups, leading to an increase of the energy of the HOMO level and hence a red shift of the emission peak position.[25,28] In fact, one may notice that, after reactions with an excess of TBAF, the PL characteristics (exaction and emission peak energies) of the Pt–EPBAPE nanoparticles started to resemble those of platinum nanoparticles functionalized with 4-ethylphenylacetylene (Pt–EPA, Scheme 1C), as depicted in Figure S2.[20]

With the addition of $TBAH_2PO_4$ and TBAI, whereas the quenching of the nanoparticle PL was apparent, the origin was most likely different. These two anions are known to adsorb rather strongly on platinum surfaces.[29,30] Thus, it is most likely that the diminishment of the nanoparticle PL intensity was due to partial desorption of EPBAPE ligands from the nanoparticle surface. In fact, precipitation of nanoparticles was observed with the addition of a large excess of these anions into the nanoparticle solution.

The high sensitivity and selectivity of the PL quenching of the Pt–EPBAPE nanoparticles by $F^-$ can be further manifested by the Stern–Volmer analysis,[31]

$$\frac{I_0}{I} - 1 = K[\mathrm{A}] \quad (1)$$

where $I_0$ and $I$ are the nanoparticle PL intensities in the absence and presence of quencher A, respectively, [A] is the concentration of quencher A, and $K$ is the Stern–Volmer quenching constant. Figure 5 depicts the Stern–Volmer plots

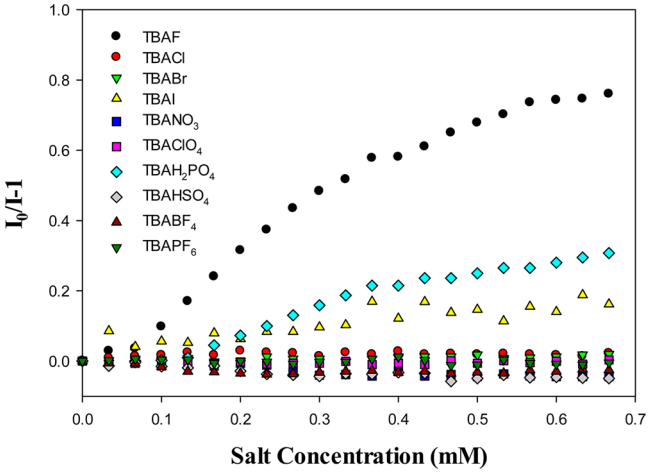


**Figure 5.** Stern–Volmer plots of the photoluminescence emission intensity of Pt–EPBAPE nanoparticles with the addition of various amounts of tetrabutylammonium salts.

in the presence of various tetrabutylammonium salts at concentrations up to 0.67 mM. There are at least two aspects that warrant attention. First, the Pt–EPBAPE nanoparticle exhibited almost linear diminishment of the photoluminescence intensity in the low anion concentration regime, and the quenching constant varies significantly with the specific quencher, as manifested by the slopes of the Stern–Volmer plots, which are summarized in Table 1. One can see that the quenching constant for $F^-$ is estimated to be $1.71 \times 10^3\ M^{-1}$, more than 3 times that of $H_2PO_4^-$ ($0.53 \times 10^3\ M^{-1}$), 6 times that of $I^-$ ($0.28 \times 10^3\ M^{-1}$), and about 2 orders of magnitude greater than those of $Br^-$ ($0.029 \times 10^3\ M^{-1}$), $Cl^-$ ($0.010 \times 10^3\ M^{-1}$), and $ClO_4^-$ ($0.008 \times 10^3\ M^{-1}$). For the rest of the series ($NO_3^-$, $HSO_4^-$, $BF_4^-$, and $PF_6^-$), the nanoparticle PL was virtually unchanged, and thus the quenching constant was essentially zero. Second, the lowest anion concentration that leads to an observable change of the nanoparticle PL intensity also varies markedly, which is estimated to be 0.051 mM for $F^-$, 0.12 mM for $H_2PO_4^-$, and 0.20 mM for $I^-$ (the rest was not measured as the nanoparticle PL was virtually unchanged). Taken together, these observations highlight the specific binding of $F^-$ among the series of anions to the boronic acid moieties (Scheme 1B).

The specific binding of fluoride ions and the boronic acid moieties was further confirmed by $^{11}B$ NMR measurements. Figure 6 shows the $^{11}B$ NMR spectra of the Pt–EPBAPE nanoparticles in the (A) absence and (B and C) presence of various amounts of TBAF in DMF-$d_6$. From curve (A) of the Pt–EPBAPE nanoparticles alone, a relatively broad peak centered at ca. 20.9 ppm can be identified, which may be ascribed to the $sp^2$ B in the boronic acid moieties (the broad


dx.doi.org/10.1021/la5001123 | Langmuir 2014, 30, 5224−5229

Table 1. Quenching Constants ($K$, $10^3$ $M^{-1}$) of the Pt−EPBAPE Nanoparticle Photoluminescence by Tetrabutylammonium Salts

| TBAF | TBACl | TBABr | TBAI | $TBANO_3$ | $TBAClO_4$ | $TBAH_2PO_4$ | $TBAHSO_4$ | $TBABF_4$ | $TBAPF_6$ |
|---|---|---|---|---|---|---|---|---|---|
| 1.71 | 0.010 | 0.029 | 0.21 | 0 | 0.008 | 0.53 | 0 | 0 | 0 |

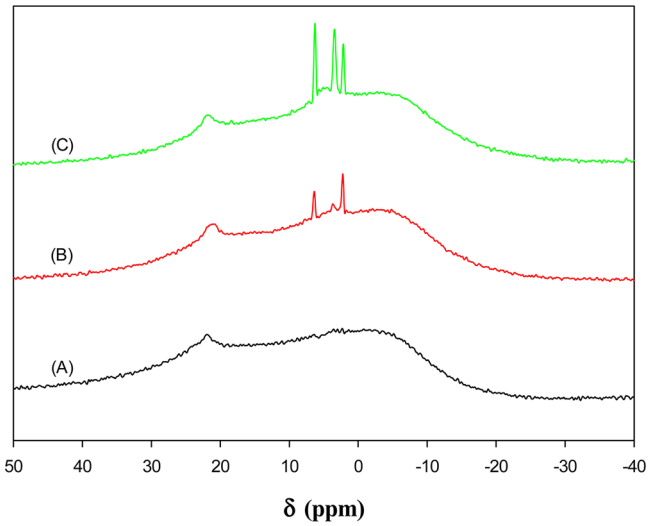


Figure 6. $^{11}B$ NMR spectra of Pt−EPBAPE nanoparticles at a concentration of 37.5 mg/mL in DMF-$d_6$ in the (A) absence and presence of various amounts of TBAF: (B) 42.4 mM and (C) 277.3 mM.

feature from 40 to −20 ppm is due to boron residuals in the NMR glass tubing).[18,30,32−35] Upon the addition of TBAF into the nanoparticle solution, the intensity of this peak diminished, and concurrently several new spectral features started to appear within the range of 6.3−2.2 ppm, which might be ascribed to B $sp^3$, and the intensity became increasingly intensified with the amount of TBAF added from 42.4 mM in curve (B) to 277.3 mM in curve (C). These behaviors are consistent with the binding of nucleophilic $F^-$ to the empty p orbitals of the boron center of the boronic acid such that the boron centers now became $sp^3$ hybridized (Scheme 1B).[33,35,36]

## CONCLUSIONS

In this study, platinum nanoparticles functionalized with ethynylphenylboronic acid panicol ester were synthesized by taking advantage of the self-assembly of acetylene moieties onto platinum surfaces forming Pt−C≡ bonds. The resulting nanoparticles exhibited apparent photoluminescence as a result of the conjugated metal−ligand interfacial bonds whereby the particle-bound acetylene moieties behaved analogously to diacetylene derivatives. Interestingly, the addition of fluoride ions led to apparent diminishment of the nanoparticle photoluminescence. This was accounted for by the specific affinity of fluoride ions to the boronic acid moieties forming stable B−F bonds that impacted the intraparticle charge delocalization. In contrast, significantly less or virtually no change of the nanoparticle photoluminescence was observed with a series of other anions that included $Cl^-$, $Br^-$, $I^-$, $NO_3^-$, $HSO_4^-$, $H_2PO_4^-$, $ClO_4^-$, $BF_4^-$, and $PF_6^-$, signifying the high selectivity of the nanoparticles toward fluoride ions. The results further highlight the significance of deliberate functionalization of nanoparticle surface in the manipulation of nanoparticle optical and electronic properties.

## ASSOCIATED CONTENT

### Supporting Information

Photoluminescence profiles of Pt−EPBAPE nanoparticles in the presence of other tetrabutylammonium salts as well as of Pt−EPA nanoparticles. This material is available free of charge via the Internet at http://pubs.acs.org.

## AUTHOR INFORMATION

### Corresponding Author

*E-mail: shaowei@ucsc.edu (S.W.C.).

### Author Contributions

The manuscript was written through contributions of all authors. All authors have given approval to the final version of the manuscript.

### Notes

The authors declare no competing financial interest.

## ACKNOWLEDGMENTS

This work was supported, in part, by the National Science Foundation (CHE-1012258 and CHE-1265635). TEM studies were carried out at the National Center for Electron Microscopy, Lawrence Berkeley National Laboratory, as part of a user project.

## REFERENCES

(1) Jeong, Y.; Patra, D.; Sanyal, A.; Rotello, V. M. Fabrication of Stable Nanoparticle-Based Colloidal Microcapsules. *Curr. Org. Chem.* **2013**, *17*, 49−57.

(2) Thaxton, C. S.; Rosi, N. L.; Mirkin, C. A. Optically and chemically encoded nanoparticle materials for DNA and protein detection. *MRS Bull.* **2005**, *30*, 376−380.

(3) Sardar, R.; Funston, A. M.; Mulvaney, P.; Murray, R. W. Gold Nanoparticles: Past, Present, and Future. *Langmuir* **2009**, *25*, 13840−13851.

(4) Perez-Juste, J.; Pastoriza-Santos, I.; Liz-Marzan, L. M.; Mulvaney, P. Gold nanorods: Synthesis, characterization and applications. *Coord. Chem. Rev.* **2005**, *249*, 1870−1901.

(5) Segev-Bar, M.; Haick, H. Flexible Sensors Based on Nanoparticles. *ACS Nano* **2013**, *7*, 8366−8378.

(6) Chen, W.; Chen, S. W.; Ding, F. Z.; Wang, H. B.; Brown, L. E.; Konopelski, J. P. Nanoparticle-mediated intervalence transfer. *J. Am. Chem. Soc.* **2008**, *130*, 12156−12162.

(7) Chen, W.; Zuckerman, N. B.; Lewis, J. W.; Konopelski, J. P.; Chen, S. W. Pyrene-Functionalized Ruthenium Nanoparticles: Novel Fluorescence Characteristics from Intraparticle Extended Conjugation. *J. Phys. Chem. C* **2009**, *113*, 16988−16995.

(8) Chen, W.; Zuckerman, N. B.; Kang, X. W.; Ghosh, D.; Konopelski, J. P.; Chen, S. W. Alkyne-Protected Ruthenium Nanoparticles. *J. Phys. Chem. C* **2010**, *114*, 18146−18152.

(9) Kang, X.; Zuckerman, N. B.; Konopelski, J. P.; Chen, S. Alkyne-functionalized ruthenium nanoparticles: ruthenium-vinylidene bonds at the metal-ligand interface. *J. Am. Chem. Soc.* **2012**, *134*, 1412−5.

(10) Kang, X. W.; Song, Y.; Chen, S. W. Nitrene-functionalized ruthenium nanoparticles. *J. Mater. Chem.* **2012**, *22*, 19250−19257.

(11) Kang, X.; Chen, S. Electronic conductivity of alkyne-capped ruthenium nanoparticles. *Nanoscale* **2012**, *4*, 4183−9.

(12) Chen, W.; Zuckerman, N. B.; Konopelski, J. P.; Chen, S. W. Pyrene-Functionalized Ruthenium Nanoparticles as Effective Chemosensors for Nitroaromatic Derivatives. *Anal. Chem.* **2010**, *82*, 461−465.

(13) Kang, X. W.; Chen, W.; Zuckerman, N. B.; Konopelski, J. P.; Chen, S. W. Intraparticle Charge Delocalization of Carbene-Functionalized Ruthenium Nanoparticles Manipulated by Selective Ion Binding. *Langmuir* **2011**, *27*, 12636−12641.
(14) Nishimura, T.; Xu, S. Y.; Jiang, Y. B.; Fossey, J. S.; Sakurai, K.; Bull, S. D.; James, T. D. A simple visual sensor with the potential for determining the concentration of fluoride in water at environmentally significant levels. *Chem. Commun.* **2013**, *49*, 478−480.
(15) Huang, S.; Jia, M.; Xie, Y.; Wang, J.; Xu, W.; Fang, H. The Progress of Selective Fluorescent Chemosensors by Boronic Acid. *Curr. Med. Chem.* **2012**, *19*, 2621−2637.
(16) Mader, H. S.; Wolfbeis, O. S. Boronic acid based probes for microdetermination of saccharides and glycosylated biomolecules. *Microchim. Acta* **2008**, *162*, 1−34.
(17) Wang, W.; Gao, X. M.; Wang, B. H. Boronic acid-based sensors. *Curr. Org. Chem.* **2002**, *6*, 1285−1317.
(18) Galbraith, E.; James, T. D. Boron based anion receptors as sensors. *Chem. Soc. Rev.* **2010**, *39*, 3831−3842.
(19) Xu, Z.; Kim, S. K.; Han, S. J.; Lee, C.; Kociok-Kohn, G.; James, T. D.; Yoon, J. Ratiometric Fluorescence Sensing of Fluoride Ions by an Asymmetric Bidentate Receptor Containing a Boronic Acid and Imidazolium Group. *Eur. J. Org. Chem.* **2009**, 3058−3065.
(20) Liu, K.; Kang, X. W.; Zhou, Z. Y.; Song, Y.; Lee, L. J.; Tian, D.; Chen, S. W. Platinum nanoparticles functionalized with acetylene derivatives: Electronic conductivity and electrocatalytic activity in oxygen reduction. *J. Electroanal. Chem.* **2013**, *688*, 143−150.
(21) Kaesz, H. D.; Saillant, R. B. Hydride Complexes of Transition-Metals. *Chem. Rev.* **1972**, *72*, 231−281.
(22) Badescu, S. C.; Jacobi, K.; Wang, Y.; Bedurftig, K.; Ertl, G.; Salo, P.; Ala-Nissila, T.; Ying, S. C. Vibrational states of a H monolayer on the Pt(111) surface. *Phys. Rev. B* **2003**, *68*, 205401-1.
(23) Dusemund, C.; Sandanayake, K. R. A. S.; Shinkai, S. Selective fluoride recognition with ferroceneboronic acid. *J. Chem. Soc., Chem. Commun.* **1995**, 333.
(24) Cooper, C. R. Selective fluorescence detection of fluoride using boronic acids. *Chem. Commun.* **1998**, 1365−1366.
(25) Nicolas, M.; Fabre, B.; Chapuzet, J. M.; Lessard, J.; Simonet, J. Boronic ester-substituted triphenylamines as new Lewis base-sensitive redox receptors. *J. Electroanal. Chem.* **2000**, *482*, 211−216.
(26) Melaimi, M.; Gabbai, F. P. A heteronuclear bidentate Lewis acid as a phosphorescent fluoride sensor. *J. Am. Chem. Soc.* **2005**, *127*, 9680−9681.
(27) Liu, X. Y.; Bai, D. R.; Wang, S. Charge-Transfer Emission in Nonplanar Three-Coordinate Organoboron Compounds for Fluorescent Sensing of Fluoride. *Angew. Chem.* **2006**, *118*, 5601−5604.
(28) Oehlke, A.; Auer, A. A.; Jahre, I.; Walfort, B.; Ruffer, T.; Zoufala, P.; Lang, H.; Spange, S. Nitro-substituted stilbeneboronate pinacol esters and their fluoro-adducts. Fluoride ion induced polarity enhancement of arylboronate esters. *J. Org. Chem.* **2007**, *72*, 4328−4339.
(29) Gisbert, R.; Garcia, G.; Koper, M. T. M. Adsorption of phosphate species on poly-oriented Pt and Pt(111) electrodes over a wide range of pH. *Electrochim. Acta* **2010**, *55*, 7961−7968.
(30) Shu, Z. X.; Bruckenstein, S. Iodine Adsorption Studies at Platinum. *J. Electroanal. Chem.* **1991**, *317*, 263−277.
(31) Lakowicz, J. R. *Principles of fluorescence spectroscopy*, 3rd ed.; Springer: New York, 2006.
(32) Phillips, W. D.; Miller, H. C.; Muetterties, E. L. B11 Magnetic Resonance Study of Boron Compounds. *J. Am. Chem. Soc.* **1959**, *81*, 4496−4500.
(33) Mooney, E. F.; Winson, P. H. Self-Association of Dibenzyl Phenylboronate. *Chem. Commun.* **1967**, 341−&.
(34) Kubo, Y.; Kobayashi, A.; Ishida, T.; Misawa, Y.; James, T. D. Detection of anions using a fluorescent alizarin-phenylboronic acid ensemble. *Chem. Commun.* **2005**, 2846−2848.
(35) Reetz, M. T.; Niemeyer, C. M.; Harms, K. Crown Ethers with a Lewis Acidic Center - a New Class of Heterotopic Host Molecules. *Angew. Chem., Int. Ed.* **1991**, *30*, 1472−1474.
(36) Galbraith, E.; James, T. D. Boron based anion receptors as sensors. *Chem. Soc. Rev.* **2010**, *39*, 3831−3842.